



Published in final edited form as:

Lab Invest. 2012 December ; 92(12): 1749–1759. doi:10.1038/labinvest.2012.141.

Lack of MMP10 exacerbates experimental colitis and promotes development of inflammation-associated colonic dysplasia

Felicitas L. Koller¹, E. Ashley Dozier², Ki Taek Nam^{1,3,4}, Mei Swee⁵, Timothy P. Birkland⁵, William C. Parks⁵, and Barbara Fingleton²

¹Department of Surgery, Vanderbilt University School of Medicine, Nashville, TN 37232

²Department of Cancer Biology, Vanderbilt University School of Medicine, Nashville, TN 37232

³Nashville Dept. of Veterans Affairs Medical Center, Vanderbilt University School of Medicine, Nashville, TN 37232

⁴Epithelial Biology Center, Vanderbilt University School of Medicine, Nashville, TN 37232

⁵Center for Lung Biology, University of Washington, Seattle, WA 98109

Abstract

Inflammatory bowel diseases such as ulcerative colitis represent serious health burdens, both because of the tissue-damaging disease itself, and because of an elevated risk of colon cancer. The increased expression of many members of the matrix metalloproteinase (MMP) family of enzymes that occurs in colitis, has long been associated with the destructive nature of the disease. Recent findings in cancer and other MMP-associated diseases, however, led us to question whether MMPs are indeed detrimental in the setting of colitis. Here, we focus on a single MMP family member, MMP10, and assess its role in a murine model of colonic tissue damage induced by dextran sulphate sodium (DSS) treatment. Using mice genetically deficient for MMP10, we find that absence of this enzyme leads to significantly worse disease scores and failure to resolve inflammation even after extended recovery periods. We show that MMP10 is produced predominantly by infiltrating myeloid cells in both murine and human colitis. Through bone marrow transplant experiments, we confirm that bone marrow-derived MMP10 contributes to colitis severity. Mice lacking MMP10 have a significantly higher propensity for development of dysplastic lesions in the colon after two rounds of DSS exposure. Thus, we conclude that MMP10 is required for resolution of DSS-induced colonic damage, and in its absence, chronic inflammation and ultimately dysplasia occurs.

Users may view, print, copy, download and text and data- mine the content in such documents, for the purposes of academic research, subject always to the full Conditions of use: http://www.nature.com/authors/editorial_policies/license.html#terms

Corresponding Author: Barbara Fingleton Ph.D., Dept of Cancer Biology, Vanderbilt University, 771 PRB, 2220 Pierce Ave, Nashville, TN 37232-6840, USA, Barbara.fingleton@vanderbilt.edu, Phone: 615-936-5877; Fax: 615-936-2912.

Disclosures

The authors have no duality of interest to declare.

Supplementary information is available at *Laboratory Investigation*'s website.

Keywords

protease; colitis; bone marrow-derived cells; resolution; cancer

Inflammatory bowel disease (IBD) affects approximately 2 million people in the US alone. Ulcerative colitis (UC), one of the most common manifestations of inflammatory bowel disease, is characterized by chronic relapsing inflammation of the large bowel that spreads from the rectum toward the colon-ileal junction. Clinical symptoms include diarrhea, rectal bleeding, passage of mucus, urgency, and abdominal pain (1). UC produces significant morbidity in affected individuals through the burden of its clinical symptoms and by increasing patients' risk of colorectal cancer (2). Histologically, UC is characterized by inflammatory cell infiltration, epithelial cell destruction, and continuous mucosal inflammation and ulceration that spread proximally from the rectum. Currently, UC is without a cure and treatment involves the administration of disease modifying agents that often carry substantial side-effects (3). Surgical treatment is also not without significant morbidity including infection, infertility, sexual dysfunction and fecal incontinence. Ideally, a treatment of UC would induce and maintain remission, promote mucosal healing, avoid surgical intervention, and reduce cancer risk (4).

Matrix metalloproteinases (MMPs) initially presented an attractive target for IBD treatment because ulcer biopsies from patients with IBD had high levels of several enzymes including MMPs-1,3,7,9, 10 and 12 (5–9). In humans, MMPs are a family of 24 proteases with unique zinc-containing catalytic domains. While there were several favorable reports on the use of synthetic MMP inhibitors in murine colitic damage induced with dextran sodium sulfate (DSS) or trinitrobenzensulfonic acid (TNBS) (10, 11), the clinical use of MMP inhibitors fell into disfavor when human cancer trials using MMP inhibitors had negative results (12).

The roles of MMPs in human disease were reappraised following the disappointing cancer trials. It became clear that MMPs had more diverse, complex functions than previously believed. In addition to matrix proteins, chemokines, cytokines, receptors and antimicrobial peptides are now recognized as *in vivo* substrates for MMPs (13, 14). The connection between MMP expression and IBD is well established, but how MMP function may be detrimental or beneficial in the course of the disease has remained unclear. A large part of the complexity stems from the myriad roles that MMPs may play *in vivo*.

Here we focus on one particular MMP, MMP10, also known as stromelysin-2. MMP 10 is a rational target for investigation in IBD because its expression has been described at healing ulcer edges in human specimens of UC (8). As is the case for many MMPs, the timing of MMP10 expression associates it with disease pathophysiology. However, the reported localization of human MMP10 to healing edges suggests a possible role in disease resolution rather than disease progression. Thus, we used *Mmp10*^{-/-} mice to ask whether MMP10 plays a beneficial or detrimental role in colonic injury using the dextran sulfate sodium (DSS) model. Further, we investigate the consequences of MMP10 ablation on the most serious long-term outcome of chronic colonic injury, i.e. neoplasia.

Materials and Methods

Mice

Breeding pairs of *Mmp10*^{-/-} mice, on the C57BL/6 background were transferred from University of Washington and used to establish colonies in both a specific-pathogen-free room (after re-derivation at Jackson Labs) and in regular mouse-housing. Similarly, C57BL/6j control mice were purchased from Jackson Labs (Bar Harbor, ME) and used to establish breeding colonies with housing in cages directly adjacent to the *Mmp10*^{-/-} colony. For all colitis experiments, 8-week old male mice were used, as female mice showed greater variation in the response to DSS (as has been reported (15)). Prior to initiation of our studies, all animal experiments were approved by the local Institutional Animal Care and Use Committee.

Experimental colitis model

A 2.5% aqueous solution of DSS (M.W. = 36,000–50,000; MP Biochemicals, Solon, OH) was provided ad libitum to the mice in water bottles for 7 days. The amount of DSS solution in the bottles was recorded daily to ensure similar exposures for all cages. After 7 days, cohorts of mice were immediately euthanized (7 day), returned to regular water for 3 days, then euthanized (10 day), returned to regular water for 7 days, then euthanized (14 day), or returned to regular water for 14 days before being euthanized (21 day). All mice were weighed daily from the first day of DSS exposure to euthanasia.

Chronic colitis

To induce a chronic colitis, mice were put through 2 separate 4-day exposures to 3% DSS that were 16 days apart. The mice were maintained for a further 4 weeks prior to euthanasia.

Bone marrow transplants

All bone marrow transplant experiments were performed with mice in the specific pathogen-free barrier facility. Bone marrow was harvested from the femurs of 4-week old donor female mice, either control C57BL/6 or *Mmp10*^{-/-}, and rinsed twice in sterile PBS. The bone marrow cells were counted and diluted with sterile PBS to a concentration of 2×10^7 cells per ml. 5-week old recipient male mice were lethally irradiated using a split dose regimen with two doses of 4 Gy given 4 hours apart, using an RS2000 Xray irradiator (RadSource, Suwanee, GA). Three hours after the second radiation dose, the mice received 2×10^6 donor bone marrow cells injected intravenously via the tail vein. Recipient mice were weighed daily for the first week following transplant and weekly thereafter until 4 weeks post-transplant. They were then administered 2.5% DSS for 7 days as described previously, switched to regular water for a 3-day recovery period and then euthanized.

Histology and Scoring

Colons were removed from euthanized mice, rinsed with PBS, then cut open longitudinally, before being rolled into 'Swiss rolls'. The Swiss rolls were held together with a 30 gauge needle, fixed in 10% formalin and embedded in paraffin. 5µm sections of the paraffin-

embedded tissue were cut and stained for basic histology using hematoxylin and eosin (H & E) and periodic acid Schiff (PAS) stains, all purchased from Sigma (St Louis, MO).

A colitis damage score was generated from digital images of PAS-stained sections, by firstly measuring the distance around the intact muscularis using the AVP Universal Desktop Ruler software. The areas of ulceration were then measured and given the following scores: 1=1/3 of the bottom of the crypt injured, 2= 2/3 of the bottom of the crypt injured, 3= total crypt loss but epithelial lining remains, 4 =crypt and epithelial loss. The ulceration was graded according to the worst area. Then, the ulceration score was multiplied by the length of involved colon. The individual ulceration scores were then summed and divided by the total colon length to give a measure of ulceration severity/unit colon. The percentage of colon scored per grade for each mouse was calculated and used to allow comparison of the spread of grades between genotypes.

Immunohistochemistry

Two different human colon tissue microarrays, both containing some specimens of human IBD were purchased from US Biomax (Rockville, MD). For mouse tissues, formalin-fixed paraffin-embedded 5µm sections were used. The slides were dewaxed, rehydrated, and treated with hydrogen peroxide to quench endogenous peroxidases. After heat-mediated antigen retrieval using 10mM sodium citrate, pH 6.0, the slides were blocked for 1 hr with 5% goat or rabbit serum and then incubated overnight with a rabbit polyclonal anti-human MMP10 antibody (Abcam, Cambridge, MA), or a rat anti-mouse neutrophil antibody (Serotec, Raleigh, NC), or a rat anti-mouse F4/80 antibody (Serotec). The following day, the slides were washed with Tris-buffered saline and incubated with biotinylated anti-rabbit or anti-rat antibodies (Vector Laboratories), before being incubated with Vectastain ABC reagent (Vector Laboratories, Burlingame, CA) following manufacturer's instructions. The chromogen diaminobezidine (DAB; Sigma) was used to visualize positive antibody binding, and the slides were counter-stained with Mayer's hematoxylin prior to clearing and mounting. Quantification of positive signals from the neutrophil and macrophage immunostaining was done using Metamorph software on images taken with a 20× objective lens with a Zeiss Axiophot microscope, as previously described.

Immunofluorescence

Colon from mice treated for 7 days with 2.5% DSS was harvested, rinsed, split open, rolled, covered with OCT freezing medium and quick frozen in liquid nitrogen. 8 micron sections were cut onto glass slides, and rinsed in PBS before fixing in acetone for 5 min and then blocking with Image-iT FX signal enhance reagent (Life Technologies, Carlsbad, CA) for 30 min followed by 10% goat serum for 15 min. The slides were incubated for 2 hr at room temperature with rat anti-F4/80 (Serotec) and/or rabbit anti-MMP10 (Novus Biologicals, Littleton, CO) in 10% serum. After washing, the slides were incubated with AlexaFluor488 anti-rat and AlexaFluor594 anti-rabbit antibodies (Life Technologies) for 30 minutes. After repeated washing and a 2 minute incubation in 0.5 µg/ml Hoechst 33258 (Sigma) diluted in PBS, the slides were mounted using Prolong Gold Anti-Fade (Life Technologies). The slides were examined with a Zeiss Axiophot microscope and 20× objective lens images captured with a Hamamatsu camera using Metamorph software.

In situ hybridization

A 750bp sequence of mouse MMP10 (16) carried in the pGem4mStr2 plasmid, a gift from Dr Lynn Matrisian, Vanderbilt University, was labeled, according to manufacturer's instructions using the Dig T7/Sp6 labeling kit (Roche Applied Bioscience, Indianapolis, IN) to produce sense and antisense probes. 5-micron paraffin sections of Swiss-rolled colons from control or DSS-exposed wild-type and *Mmp10*^{-/-} mice were dewaxed, rehydrated then post-fixed in 4% paraformaldehyde. The sections were digested with 10 µg/ml proteinase K for 20 minutes, then immersed in 0.2N HCl for 1 hour to quench endogenous alkaline phosphatase activity. Following 10 minute immersions in 0.1M triethanolamine and 0.1M triethanolamine/0.25% acetic acid, to inhibit electrostatic interactions, the sections were air-dried for several hours. For hybridization, sense or antisense probes diluted to 1.5 ng/ml with hybridization buffer (Dako Cytomation, Ventura, CA) were placed on individual sections in a humid chamber. Each section was covered with a hybri-slip (Sigma), and the chamber incubated at 50°C for 16 hours. Following hybridization, the slides were washed in three changes of 2X SSC/50% formamide at 50°C, then in 2X SSC at room temperature. The presence of probe was detected using an alkaline phosphatase-labeled anti-digoxigenin antibody (Roche) that was incubated with the sections for 2 hours, according to manufacturer's recommendations. Following washing, colorimetric signal was developed using the substrates BCIP and NBT (Promega, Madison, WI).

Quantitative PCR

Isolation and analysis was performed as previously described (17). Briefly, total RNA was isolated using Trizol (Invitrogen, Carlsbad, CA) and used to generate cDNA with a High Capacity cDNA archive kit (Applied Biosystems, Foster City, CA). 5 µg of the cDNA was mixed with primers and FAM-labeled Taqman probes for MMP10 and GAPDH, and product was measured using an ABI- HT7900 Fast Real-Time PCR system. The threshold cycle (Ct) was obtained from duplicate samples and averaged, and the Ct range for each is shown in the figure legends. The Ct was the difference between the average Ct for the specific cDNAs and the average Ct for GAPDH, which ranged from 16.97 to 14.16. The

Ct was the average Ct at a given time point minus the average Ct of day-0 samples. The data are expressed as relative quantification (RQ), which is the fold change and calculated as $2^{-\Delta Ct}$. For measurement of macrophage markers, specific Quantitect primers for *Nos2* (iNOS), *Cxcl10*, *Ccl3*, *Chi3l3* (Ym1), *Retnla* (FIZZ), *Arg1* (arginase) and *Gapdh* were obtained from Qiagen and transcripts were detected using SYBR Green that had been included in the QuantiFast reaction mixture (Qiagen). Analysis was performed as above.

In vivo permeability measurement

An 80mg/ml solution of FITC-dextran (4000 MW; Sigma) was prepared with sterile saline and administered to 5 each control and *Mmp10*^{-/-} mice after 0 or 3 days of 2.5% DSS treatment by oral gavage at a dose of 600 mg/Kg. Four hours later, serum was collected from the gavaged mice and assayed using a fluorometric plate reader (Victor3 Multi-Label Counter, Perkin-Elmer) for levels of green fluorescence from the FITC-dextran.

Evaluation of cytokines and chemokines

Multi-array ELISA plates for both cytokines and chemokines were purchased from SA Biosciences (Frederick, MD). Pooled plasma or colonic lavage fluid from 3 each control or *Mmp10*^{-/-} mice collected at 0, 4-days or 8-days post initiation of DSS exposure were used for these assays, which were performed according to the manufacturer's instructions. Only those cytokines/chemokines that showed differences between the control and *Mmp10*^{-/-} groups were evaluated further. Single analyte ELISAs for the cytokines IL1, IFN γ , G-CSF and TNF, and the chemokine MCP-1 were purchased from SA Biosciences. Plasma or lavage fluid from individual mice collected 0,4 or 8-days post initiation of DSS-exposure were analyzed following manufacturer's recommendation.

Macrophage cell culture

RAW264.7 murine monocyte cells were obtained from American Tissue Culture Collection (ATCC, Rockville, MD) and maintained as recommended in Dulbecco's modified Eagles medium (DMEM; Life Technologies) containing 10% fetal calf serum. For activation *in vitro*, the cells were treated with 10 ng/ml lipopolysaccharide (LPS; Sigma) plus 100 IU/ml interferon- γ (R&D Systems, Minneapolis, MN) or 10ng/ml interleukin-4 (IL4; Life Technologies) plus 10 ng/ml interleukin-13 (IL13; Life Technologies) for 24 hours as previously described (Zhang).

Results

MMP-10 mRNA expression is increased in mice exposed to DSS

MMP10 is expressed by ulcer-edge enterocytes and cells within granulation tissue in human ulcerative colitis (8, 18). To assess possible function of this enzyme in colitic disease, we first determined when MMP10 is expressed in a mouse model of acute colitis. Mice were exposed to 2.5% dextran sulfate sodium (DSS) provided ad libitum in drinking water for a period of 7 days, and then returned to regular drinking water. At days 0, 7, 10, 14, 21 and 28 post-initiation of DSS, groups of mice were euthanized, and RNA prepared from the colonic tissue. As can be seen in Fig 1A, MMP10 expression was low to absent in normal colonic tissue, rose to peak expression at the end of the DSS treatment and then gradually returned to control levels. Based on Ct values greater than 35, we conclude that MMP10 was not expressed in normal colon but was induced in response to acute colon injury, and that expression is turned off once the tissue has repaired and inflammation has resolved. Semi-quantitative reverse-transcription PCR using a different set of primers confirmed these results (data not shown).

Infiltrating cells are responsible for the majority of MMP10 seen in murine and human inflammatory bowel disease

Animals exposed to 2.5% DSS predictably developed colitic damage and associated inflammation, which was histologically confirmed by crypt loss as well as infiltration of a large number of cells. Since we found antibodies to mouse MMP10 to be unreliable for immunohistochemistry in paraffin sections, we used *in situ* hybridization to identify the cell types responsible for the production of MMP-10 in colitic areas. The strongest positive

signal was seen in infiltrating cells surrounding the bottom of crypts (Fig 1B). To ascertain whether such expression was limited to the DSS acute colitis model, we also stained sections from interleukin-10 null mice, which develop spontaneous chronic inflammatory bowel disease (19). As can be seen in Fig 1C, there was a similar pattern of MMP10 positivity in infiltrating cells within colonic lesions. To determine whether the pattern of expression was similar in human inflammatory bowel disease, we examined archival de-identified human colon tissue specimens from IBD patients. While there was some evidence of epithelial expression as reported in earlier literature (18), by far the strongest expression was in inflammatory cells (Fig 1D). Overall, 6 out of 15 sections showed MMP10 staining in epithelial cells, 13 out of 15 showed MMP10 staining in inflammatory cells and 2 out of 15 had no detectable MMP10. To determine whether the MMP10-expressing cells were macrophages, as suggested by morphology, we used a double-staining immunofluorescent procedure on frozen sections of colon tissue from mice that had been exposed to 2.5% DSS for 7 days. As shown in Fig 1E, the majority of the MMP10-positive cells in the sub-crypt area also stained for the macrophage marker F4/80.

MMP-10 null mice have more severe DSS colitis

To determine the functional significance of MMP10 in acute colitis, we placed cohorts of wildtype and *Mmp10*^{-/-} mice on DSS treatment for 7 days, then allowed subgroups of each genotype to heal for different periods of time (Fig 2A). To measure the severity of DSS colitis, we monitored weight loss, colon length, and histologic score. Mice consistently reached the nadir of their weight loss at 8–10 days post DSS-initiation (Fig 2B). At the 10 day time point the weight loss of the *Mmp10*^{-/-} mice was significantly worse in the 10, 14 and 21 day groups. Notably, we observed no difference in either starting weight or colon lengths between control *Mmp10*^{-/-} and wildtype mice not exposed to DSS (Supplemental Fig 1A, B). Colon shortening, a morphometric measure of inflammation was more severe in the *Mmp10*^{-/-} mice (Supplemental Fig 2). Ulceration scores, generated from histological assessment, showed significant differences in the amount of severe, grade 4 ulceration in the *Mmp10*^{-/-} mice compared to wild-type controls (Fig 2C). In wildtype mice, there was almost complete resolution of histological damage to the colon by day 21 i.e. 14 days after discontinuation of the DSS. In contrast, significant tissue damage remained evident in *Mmp10*^{-/-} mice at this timepoint.

Basal proliferation and intestinal permeability is normal in *Mmp10*^{-/-} mice

Mmp10^{-/-} animals do not have any gross phenotypic abnormalities and reproduce normally (20). The general appearance of their colons and presence of inflammatory cells did not differ from wildtype mice (data not shown). Since it has been reported that mice deficient in a related enzyme, MMP2, appear to have a defect in barrier function in the gut (21), we assessed gut permeability directly. To do this, cohorts of wildtype and *Mmp10*^{-/-} mice received a dose of FITC-dextran by oral gavage. After 4 hours, serum was collected from the gavaged mice and the levels of FITC measured using a plate fluorometer. As anticipated from the lack of baseline inflammation, permeability did not differ between control wildtype and *Mmp10*^{-/-} mice (Supplemental Fig 3A). Notably, the permeability was increased after 3 days of exposure to 2.5% DSS but was still not significantly different between the two strains of mice (Supplemental Fig 3B). Immunohistochemical staining of the colonic tissue

also demonstrated that untreated *Mmp10*^{-/-} and wildtype animals have no difference in the number of dividing cells identified by phosphohistone-3 immunostaining (data not shown). Thus, we concluded that the differences seen following DSS exposure were not due to baseline differences between wildtype and *Mmp10*^{-/-} mice.

Leukocyte infiltration was increased in MMP10- null mice

To better characterize the infiltrating cell populations in the colonic lesions that developed after DSS exposure, we immunostained colon sections with anti-neutrophil antibody. Although at day 7 we observed fewer neutrophils in *Mmp10*^{-/-} colons, at days 10 and 14 there was a trend for greater neutrophils in *Mmp10*^{-/-} mice compared to wildtypes (Fig. 3A). More strikingly, at day 21, when neutrophilia had largely resolved in wildtype mice, elevated numbers of neutrophils persisted in the colons on *Mmp10*^{-/-} mice (Fig. 3A). In contrast, there was a significantly higher level of macrophages at day 7 in the MMP10-null samples, coincident with the peak expression of MMP10 seen in wildtype mice (Fig. 1A). Intriguingly, at day 21, although there were still large lesions visible in the *Mmp10*^{-/-} tissues, staining for F4/80+ macrophages was undetectable, similar to the situation in the healed wildtype colons. Since macrophages can be activated to different functional states, and there are suggestions that alternatively activated (M2) macrophages are important in resolution of DSS-induced damage, we assessed levels of macrophage activation markers. Whole colons were isolated from 5 each wildtype and *Mmp10*^{-/-} mice that had been exposed to 2.5% DSS for 7 days, then given one day to start recovery. Levels of transcripts for the classically activated (M1) macrophage markers INOS, CXCL3 and CCL10, as well as for the alternative activation (M2) macrophage markers mannose receptor, Ym1 and FIZZ were determined using real-time PCR analysis of RNA from the colon tissue. The combination of these markers for macrophage phenotyping has been described in the literature (22, 23). As can be seen in Fig 3C, the relative levels of M1 markers were increased while M2 markers were decreased in the colonic tissue from DSS-treated *Mmp10*^{-/-} mice.

Cytokine profiles of colonic lavage correlate with severity of colitis

Since MMP10 was primarily produced by inflammatory cells during DSS-induced colitis, we reasoned that MMP10 may play a role in cytokine release. To assess whether levels of secreted cytokines were different between wildtype and *Mmp10*^{-/-} mice, colonic lavage fluid was collected from mice that had been exposed to 3–4 or 7 days of DSS. The 7 day exposure group was given 1 additional day on regular water to allow the repair process to begin before samples were collected on day 8. Samples were also collected from mice that were never exposed to DSS. Levels of cytokines were then assessed as detailed in *Materials and Methods*. Levels of IL-1A, TNF α , and G-CSF were significantly increased in MMP10-null animals 8 days after initial exposure to DSS compared to the wildtype counterparts, however, we saw no difference in levels of any cytokine between genotypes at earlier timepoints (Fig 4A–C). In addition, the levels of other factors assayed (ILs-1b, -2, -4, -6, -10, -12, -17a; Interferon- γ ; or GM-CSF) did not differ between wildtype and *Mmp10*^{-/-} at baseline or either experimental timepoint (data not shown). Thus the higher levels of specific pro-inflammatory cytokines at the late timepoint in the *Mmp10*^{-/-} mice were most likely related to a failure to resolve on-going inflammation.

Since there was an apparent difference in the number of infiltrating leukocytes in the colitic lesions of DSS-treated *Mmp10*^{-/-} mice compared to controls, we also assessed levels of chemokines both in the local environment, by testing colonic lavage, and systemically in the blood. Only one chemokine, macrophage chemoattractant protein-1 (MCP-1/CCL2) differed between wildtype and *Mmp10*^{-/-} mice, with elevated levels in null mice at both early and late stages of disease, suggesting that it may have a functional role in inducing the exacerbated inflammatory response (Fig 4D).

Bone marrow transplant suggests marrow genotype contributes to severity of colitis

The identification of infiltrating cells, particularly macrophages, as the predominant cellular source of MMP10 prompted us to investigate whether the more severe colitic phenotype of the *Mmp10*^{-/-} mice was dependent only on bone marrow cells. We lethally irradiated matched cohorts of control and *Mmp10*^{-/-} animals and repopulated with donor marrow from healthy control or *Mmp10*^{-/-} mice. After a 4-week period of reconstitution, we challenged recipient mice with a seven-day course of 2.5% DSS and then euthanized mice one day after the DSS treatment ended. Analysis of weights showed no significant differences amongst the groups (Fig 5A). Histological analysis, however, indicated that the extent of grade 4 severe lesions was associated predominantly with the genotype of the bone marrow supplied in *Mmp10*^{-/-} but not wildtype recipient mice (Fig 5B). It is important to note that these experiments were conducted in a specific pathogen-free barrier facility, where the severity of DSS-induced colitis was reduced in all animals compared to their counterparts in normal housing. Overall, these results suggest that bone marrow-derived MMP10 contributes to amelioration of colitis severity, but other cellular sources present in wild-type mice are also important.

Incidence of dysplasia is increased in *Mmp10*^{-/-} mice

In order to determine whether lack of MMP10 altered colitis-associated cancer development, we attempted to induce chronic colitis by repeated exposure to DSS. Previous literature demonstrated that 4 rounds of DSS exposure result in chronic colitis in C57BL/6 mice (24). However, severe morbidity that reached the criteria for euthanasia occurred in the *Mmp10*^{-/-} mice after only 2 rounds of DSS, barring any further exposure. Thus, we treated cohorts of wild-type and *Mmp10*^{-/-} mice with two 4-day rounds of 3% DSS, 3 weeks apart, and let the animals recover for a further 3 weeks before termination. We then isolated the colons and examined them histologically. As expected, the degree of dysplasia in the wild-type mice after only 2 rounds of DSS was very low. In *Mmp10*^{-/-} mice, however, the frequency of dysplasias detected was significantly elevated (6/8 (75.0%) in *Mmp10*^{-/-} versus 1/7 (14.3%) in wildtype; $p = 0.04$, Chi-square test). Examples of the lesions detected in *Mmp10*^{-/-} mice are shown in Fig 6.

Discussion

Here we have used the DSS model of acute intestinal damage and inflammation to investigate functions of the proteinase MMP10. Although MMP10 expression was induced in response to colon injury, our data indicate that this proteinase functions more in disease resolution than progression. Mice lacking MMP10 were clearly deficient in their ability to

effectively heal mucosal ulcers. These results lead us to characterize MMP10 as playing a beneficial/protective role in the DSS-induced colitic damage model, and suggest that strategies to enhance MMP10 rather than inhibit its activity may have therapeutic impact.

One difficulty with testing possible molecular mechanisms for IBD and associated therapeutic strategies is the paucity of models that can truly recapitulate the complexity of human disease. Nevertheless, particular aspects of the disease process such as immune cell dysregulation or epithelial damage can be examined using the IL-10^{-/-} mouse (19), transplantation of CD45^{hi} CD4⁺ T cells into immunosuppressed animals (25) or treatment with agents such as trinitrobenzenesulfonic acid (TNBS) (26) or dextran sulfate sodium (DSS) (27), respectively. The DSS model, in particular, is widely used because of the ease of administration and ability for temporal control (27). The detailed mechanism by which DSS induces damages and ensuing acute inflammation has been recently described (28). One attractive feature of this model is different strains of mice and other rodents are differentially sensitive to the effects of DSS, reflecting the role that genetic factors have in human disease (15). Thus, although the DSS model cannot be considered “mouse ulcerative colitis”, aspects of it are similar and it has been useful in identifying some important pathways as well as for testing of drugs (27).

A previous report of MMP10 in human inflammatory bowel disease suggested a possible role in healing, however this was based solely on apparent localization in migrating epithelial cells (18). Our investigation of MMP10 localization in DSS-injured and IL10-null mouse colons and in human IBD samples revealed more prominent expression in leukocytes rather than epithelial cells, a pattern also seen in models of lung infection and injury (WCP, unpublished observations). From their morphology, the MMP10-positive cells were of a monocytic origin. In the DSS model, we then confirmed macrophage expression of MMP10 using co-staining with the widely-used murine macrophage marker F4/80 (29). Although F4/80 is predominantly expressed by macrophages, there can be some expression by subclasses of dendritic cells and eosinophilic granulocytes, therefore there remains a formal possibility that myeloid cells other than macrophages express MMP10 in the DSS model. Our bone marrow transplant experiments support the premise that MMP10 in bone marrow-derived cells provides a protective response to DSS-induced injury. This is most clearly shown when the bone marrow is transplanted to *Mmp10*^{-/-} recipients. Since the effect is not so clear in wild-type mice, MMP10 from non-bone marrow derived cells must also contribute to regulation of colitis severity.

As MMPs are often thought of as extracellular matrix-degrading enzymes, it is unsurprising that they are often thought of as being destructive. Indeed many previous studies of MMPs in several colitis models have confirmed deleterious functions (10, 11, 30–33). A common strategy for such studies was the administration of broad-spectrum MMP inhibitor drugs to experimental animals, and observation of disease modification. However, such an approach can obfuscate differential roles for individual family members. An alternative approach has been the use of *in vivo* administered silencing RNAs (siRNAs) toward individual members. Such reagents have been used to target both MMP3 and MMP10 in DSS-induced colitis (34), however the level of knockdown achieved (approximately 50%), the length of time for which knockdown is achieved, and the unknown penetration of the knockdown into different

cell types means that results are very difficult to interpret. The availability of mouse lines genetically ablated for specific MMPs has allowed more careful probing of the contributions of particular enzymes (35). For example, the gelatinases MMP2 and MMP9 appear to have opposing roles with MMP9 being destructive and MMP2 protective due to effects on maintenance of intestinal barrier function (21). Protective functions for individual family members have also been seen in other disease settings such as cancer (36, 37). Indeed, the same MMP can have both protective and destructive roles that are context-dependent (36). Together, these findings illustrate that the once popular therapeutic strategy of broad MMP inhibition is flawed. Our data would suggest that MMP10 inhibition is likely to enhance disease severity and increase healing time. It remains to be seen if increasing the levels of MMP10 would have the opposite effect and reduce healing time. If so, this could prove a valuable tool in minimizing the clinical problems associated with IBD.

One of the most dangerous effects of chronic IBD is the increased risk for colon cancer development. Colitis-associated colon cancer, while in many ways similar to sporadic colon cancer, does have some particular characteristics. It is associated with younger age at onset, a mucinous/signet ring histology, a higher rate of 2 or more synchronous primary tumors, and a more proximal distribution in the colon (2). In the setting of IBD, cancers are believed to progress from no dysplasia to “indefinite” dysplasia, to low grade, then high grade dysplasia ultimately becoming carcinoma (2). In our studies, a lack of MMP10 resulted in enhanced development of dysplasia in DSS-treated mice. While we cannot rule out direct MMP10-mediated changes in epithelial cells, the most likely explanation is that the unremitting inflammation seen in DSS-treated *Mmp10*^{-/-} mice is the major cause. In other mouse models of colon cancer such as *Apc*^{Min/+}, as well as in human colon cancer specimens, MMP10 levels are often increased (38, 39), although this is in multiple cell types including epithelial tumor cells. It is as yet unclear if the enzyme contributes to cancer progression or if its increased levels are merely an indicator of increased numbers of cancer cells. Future studies will address possible roles of MMP10 in colorectal cancer development and progression.

A major question remaining from our studies is the identification of the MMP10 substrate(s) responsible for its protective function. Since persistent inflammation is the dominant phenotype associated with MMP10 loss in both this study and in a previously published *Pseudomonas aeruginosa* infection model (20), cleavage of a cytokine/chemokine may be responsible for regulating immune response. MMP-mediated processing of chemokines has been reported in several systems (14) and other studies have shown MMP-dependent effects on chemokine compartmentalization (40, 41). Such modifications usually produce proteins reduced in only a small number of amino acids, so these changes are unlikely to be detected using ELISA methodologies such as were used here. We did find a change in the circulating levels of monocyte chemoattractant protein (MCP)-1 at early timepoints post-DSS treatment that suggest this may be an important effector of the enhanced inflammatory response in *Mmp10*^{-/-} mice. It should be noted, however, that there are no apparent disease differences between the wildtype and *Mmp10*^{-/-} mice at early timepoints after DSS exposure. Intestinal permeability is similarly increased between the two genotypes compared to their baseline counterparts (Supp Fig 3B), and a pilot study assessing histological changes also showed no

quantifiable difference between the genotypes after 4 days of DSS exposure (data not shown).

While increased inflammation was evident in the DSS-treated *Mmp10*^{-/-} mice, and neutrophil numbers were particularly high, the numbers of F4/80-positive macrophages decreased over time in DSS-treated *Mmp10*^{-/-} mice compared to the corresponding wild-type mice. Interestingly, the phenotype of the DSS-treated *Mmp10*^{-/-} mice is strikingly similar to one reported by Qualls and colleagues in which macrophages were either systemically or locally depleted (42). More recently, CX3CR1-deficient mice were shown to have significant reduction in lamina propria macrophages and have enhanced severity of DSS-induced colitis (43). Other studies have suggested that macrophages are required for wound healing in models of colonic damage (44, 45). Finally, there are indications that alternatively activated or M2 macrophages can be protective against colitis induced by either TNBS (46) or DSS (47). In our study, not only are macrophage numbers lower in *Mmp10*^{-/-} mice, but there appears to be a skewing toward M1 rather than M2 macrophages. Overall then, the changes in macrophages seen in DSS-treated *Mmp10*^{-/-} mice are likely contributing factors to the failure of the healing program in these mice.

In conclusion, the data presented here indicate that MMP10, produced by infiltrating myeloid cells after DSS-induced colonic damage, plays a role in disease resolution. In the absence of this enzyme, colonic inflammation persists and eventually results in the development of dysplastic lesions. Thus, enhancing MMP10 expression may be a therapeutic strategy worth considering for promotion of mucosal healing.

Supplementary Material

Refer to Web version on PubMed Central for supplementary material.

Acknowledgements

We are especially thankful to Dr Mark Frey of the University of Southern California for paraffin sections from H110-null mice, to Dr Lynn Matrisian for the MMP10 *in situ* hybridization probe, and to the Vanderbilt Tissue Acquisition Core for the archival de-identified human IBD specimens. Additionally, we gratefully acknowledge Dr M. K. Washington for helpful discussions regarding histology scoring, and Dr J.T.Roland and the Epithelial Biology Center Shared Imaging Resource for Ariol scanning of slides.

Funding: FLK was supported by training grant T32CA106183. This work was also supported by the Vanderbilt-Ingram Cancer Center support grant P30CA068485, by pilot funding from the Vanderbilt Digestive Disease Research Center P30DK058404, and by HL089455 and HL098067 (WCP)

Abbreviations

MMP	matrix metalloproteinase
MMP10	matrix metalloproteinase-10
DSS	dextran sulfate sodium
MCP-1	monocyte chemoattractant protein-1
UC	ulcerative colitis

IBD	inflammatory bowel disease
TNF-α	tumor necrosis factor-alpha
G-CSF	Granulocyte-colony stimulating factor
IL-1	interleukin-1

References

- Osterman, MT.; Lichtenstein, GR. Chapter 112 - Ulcerative Colitis. In: Feldman, M.; Friedman, LS.; Brandt, L.J., editors. *Sleisenger's and Fordtran's Gastrointestinal and Liver Disease*. 9th ed.. Philadelphia, PA: Saunders; 2010. p. 1982
- Itzkowitz SH, Yio X. Inflammation and cancer IV. Colorectal cancer in inflammatory bowel disease: the role of inflammation. *Am J Physiol Gastrointest Liver Physiol*. 2004; 287:G7–G17. [PubMed: 15194558]
- Sandborn WJ, Loftus EV. Balancing the risks and benefits of infliximab in the treatment of inflammatory bowel disease. *Gut*. 2004; 53:780–782. [PubMed: 15138201]
- Ng SC, Kamm MA. Therapeutic strategies for the management of ulcerative colitis. *Inflamm Bowel Dis*. 2009; 15:935–950. [PubMed: 18985710]
- Baugh MD, Perry MJ, Hollander AP, et al. Matrix metalloproteinase levels are elevated in inflammatory bowel disease. *Gastroenterology*. 1999; 117:814–822. [PubMed: 10500063]
- von Lampe B, Barthel B, Coupland SE, et al. Differential expression of matrix metalloproteinases and their tissue inhibitors in colon mucosa of patients with inflammatory bowel disease. *Gut*. 2000; 47:63–73. [PubMed: 10861266]
- Matsuno K, Adachi Y, Yamamoto H, et al. The expression of matrix metalloproteinase matrilysin indicates the degree of inflammation in ulcerative colitis. *J Gastroenterol*. 2003; 38:348–354. [PubMed: 12743774]
- Vaalamo M, Karjalainen-Lindsberg ML, Puolakkainen P, et al. Distinct expression profiles of stromelysin-2 (MMP-10), collagenase-3 (MMP-13), macrophage metalloelastase (MMP-12), and tissue inhibitor of metalloproteinases-3 (TIMP-3) in intestinal ulcerations. *Am J Pathol*. 1998; 152:1005–1014. [PubMed: 9546361]
- Saarialho-Kere UK, Vaalamo M, Puolakkainen P, et al. Enhanced expression of matrilysin, collagenase, and stromelysin-1 in gastrointestinal ulcers. *Am J Pathol*. 1996; 148:519–526. [PubMed: 8579114]
- Di Sebastiano P, di Mola FF, Artese L, et al. Beneficial effects of Batimastat (BB-94), a matrix metalloproteinase inhibitor, in rat experimental colitis. *Digestion*. 2001; 63:234–239. [PubMed: 11435723]
- Sykes AP, Bhogal R, Brampton C, et al. The effect of an inhibitor of matrix metalloproteinases on colonic inflammation in a trinitrobenzenesulphonic acid rat model of inflammatory bowel disease. *Aliment Pharmacol Ther*. 1999; 13:1535–1542. [PubMed: 10571613]
- Coussens LM, Fingleton B, Matrisian LM. Matrix metalloproteinase inhibitors and cancer: trials and tribulations. *Science*. 2002; 295:2387–2392. [PubMed: 11923519]
- Egeblad M, Werb Z. New functions for the matrix metalloproteinases in cancer progression. *Nature Revs Cancer*. 2002; 2:161–174. [PubMed: 11990853]
- Parks WC, Wilson CL, Lopez-Boado YS. Matrix metalloproteinases as modulators of inflammation and innate immunity. *Nature Revs Immunol*. 2004; 4:617–629. [PubMed: 15286728]
- Mähler M, Bristol IJ, Leiter EH, et al. Differential susceptibility of inbred mouse strains to dextran sulfate sodium-induced colitis. *Am J Physiol*. 1998; 274:G544–G551. [PubMed: 9530156]
- Gack S, Vallon R, Schmidt J, et al. Expression of interstitial collagenase during skeletal development of the mouse is restricted to osteoblast-like cells and hypertrophic chondrocytes. *Cell Growth Differ*. 1995; 6:759–767. [PubMed: 7669731]

17. Swee M, Wilson CL, Wang Y, et al. Matrix metalloproteinase-7 (matrilysin) controls neutrophil egress by generating chemokine gradients. *J Leukoc Biol.* 2008; 83:1404–1412. [PubMed: 18334539]
18. Salmela MT, Pender SL, Karjalainen-Lindsberg ML, et al. Collagenase-1 (MMP-1), matrilysin-1 (MMP-7), and stromelysin-2 (MMP-10) are expressed by migrating enterocytes during intestinal wound healing. *Scand J Gastroenterol.* 2004; 39:1095–1104. [PubMed: 15545168]
19. Kuhn R, Lohler J, Rennick D, et al. Interleukin-10-deficient mice develop chronic enterocolitis. *Cell.* 1993; 75:263–274. [PubMed: 8402911]
20. Kassim SY, Gharib SA, Mecham BH, et al. Individual matrix metalloproteinases control distinct transcriptional responses in airway epithelial cells infected with *Pseudomonas aeruginosa*. *Infect Immun.* 2007; 75:5640–5650. [PubMed: 17923522]
21. Garg P, Rojas M, Ravi A, et al. Selective ablation of matrix metalloproteinase-2 exacerbates experimental colitis: contrasting role of gelatinases in the pathogenesis of colitis. *J Immunol.* 2006; 177:4103–4112. [PubMed: 16951375]
22. Wang Y, Wang YP, Zheng G, et al. Ex vivo programmed macrophages ameliorate experimental chronic inflammatory renal disease. *Kidney Int.* 2007; 72:290–299. [PubMed: 17440493]
23. Zaynagetdinov R, Sherrill TP, Polosukhin VV, et al. A critical role for macrophages in promotion of urethane-induced lung carcinogenesis. *J Immunol.* 2011; 187:5703–5711. [PubMed: 22048774]
24. Clapper ML, Cooper HS, Chang WC. Dextran sulfate sodium-induced colitis-associated neoplasia: a promising model for the development of chemopreventive interventions. *Acta pharmacologica Sinica.* 2007; 28(9):1450–1459. [PubMed: 17723178]
25. Kim HS, Berstad A. Experimental colitis in animal models. *Scand J Gastroenterol.* 1992; 27:529–537. [PubMed: 1641579]
26. te Velde AA, Verstege MI, Hommes DW. Critical appraisal of the current practice in murine TNBS-induced colitis. *Inflamm Bowel Dis.* 2006; 12:995–999. [PubMed: 17012970]
27. Perse M, Cerar A. Dextran sodium sulphate colitis mouse model: traps and tricks. *J Biomed Biotech.* 2012; 2012:718617.
28. Laroui H, Ingersoll SA, Liu HC, et al. Dextran sodium sulfate (DSS) induces colitis in mice by forming nano-lipocomplexes with medium-chain-length fatty acids in the colon. *PLoS One.* 2012; 7:e32084. [PubMed: 22427817]
29. van den Berg TK, Kraal G. A function for the macrophage F4/80 molecule in tolerance induction. *Trends Immunol.* 2005; 26(10):506–509. [PubMed: 16087400]
30. Medina C, Santana A, Llopis M, et al. Induction of colonic transmural inflammation by *Bacteroides fragilis*: implication of matrix metalloproteinases. *Inflamm Bowel Dis.* 2005; 11:99–105. [PubMed: 15677902]
31. Medina C, Santana A, Paz MC, et al. Matrix metalloproteinase-9 modulates intestinal injury in rats with transmural colitis. *J Leukoc Biol.* 2006; 79:954–962. [PubMed: 16478919]
32. Medina C, Santana A, Paz-Cabrera MC, et al. Increased activity and expression of gelatinases in ischemic colitis. *Dig Dis Sci.* 2006; 51:2393–2399. [PubMed: 17089188]
33. Naito Y, Yoshikawa T. Role of matrix metalloproteinases in inflammatory bowel disease. *Mol Aspects Med.* 2005; 26:379–390. [PubMed: 16112187]
34. Kobayashi K, Arimura Y, Goto A, et al. Therapeutic implications of the specific inhibition of causative matrix metalloproteinases in experimental colitis induced by dextran sulphate sodium. *J Pathol.* 2006; 209:376–383. [PubMed: 16552705]
35. Gill SE, Kassim SY, Birkland TP, et al. Mouse Models of MMP and TIMP Function. *Methods Mol Biol.* 2010; 622:31–52. [PubMed: 20135274]
36. Overall CM, Kleinfeld O. Tumour microenvironment - opinion: validating matrix metalloproteinases as drug targets and anti-targets for cancer therapy. *Nat Rev Cancer.* 2006; 6:227–239. [PubMed: 16498445]
37. Martin MD, Matrisian LM. The other side of MMPs: Protective roles in tumor progression. *Cancer Metastasis Rev.* 2007; 26:717–724. [PubMed: 17717634]
38. Sinnamon MJ, Carter KJ, Sims LP, et al. A protective role of mast cells in intestinal tumorigenesis. *Carcinogenesis.* 2008; 29:880–886. [PubMed: 18258601]

39. Sabates-Bellver J, Van der Flier LG, de Palo M, et al. Transcriptome profile of human colorectal adenomas. *Mol Cancer Res.* 2007; 5:1263–1275. [PubMed: 18171984]
40. Li O, Park PW, Wilson CL, et al. Matrilysin shedding of syndecan-1 regulates chemokine mobilization and transepithelial efflux of neutrophils in acute lung injury. *Cell.* 2002; 111:635–646. [PubMed: 12464176]
41. Corry DB, Rishi K, Kanellis J, et al. Decreased allergic lung inflammatory cell egression and increased susceptibility to asphyxiation in MMP2-deficiency. *Nat Immunol.* 2002; 3:347–353. [PubMed: 11887181]
42. Qualls JE, Kaplan AM, van Rooijen N, et al. Suppression of experimental colitis by intestinal mononuclear phagocytes. *J Leukoc Biol.* 2006; 80:802–815. [PubMed: 16888083]
43. Medina-Contreras O, Geem D, Laur O, et al. CX3CR1 regulates intestinal macrophage homeostasis, bacterial translocation, and colitogenic Th17 responses in mice. *J Clin Invest.* 2011; 121:4787–4795. [PubMed: 22045567]
44. Pull SL, Doherty JM, Mills JC, et al. Activated macrophages are an adaptive element of the colonic epithelial progenitor niche necessary for regenerative responses to injury. *Proc Natl Acad Sci USA.* 2005; 102:99–104. [PubMed: 15615857]
45. Seno H, Miyoshi H, Brown SL, et al. Efficient colonic mucosal wound repair requires Trem2 signaling. *Proc Natl Acad Sci USA.* 2009; 106:256–261. [PubMed: 19109436]
46. Rizzo A, Monteleone I, Fina D, et al. Inhibition of colitis by IL-25 associates with induction of alternatively activated macrophages. *Inflamm Bowel Dis.* 2012; 18:449–459. [PubMed: 21688353]
47. Weisser SB, Brugger HK, Voglmaier NS, et al. SHIP-deficient, alternatively activated macrophages protect mice during DSS-induced colitis. *J Leukoc Biol.* 2011; 90:483–492. [PubMed: 21685246]

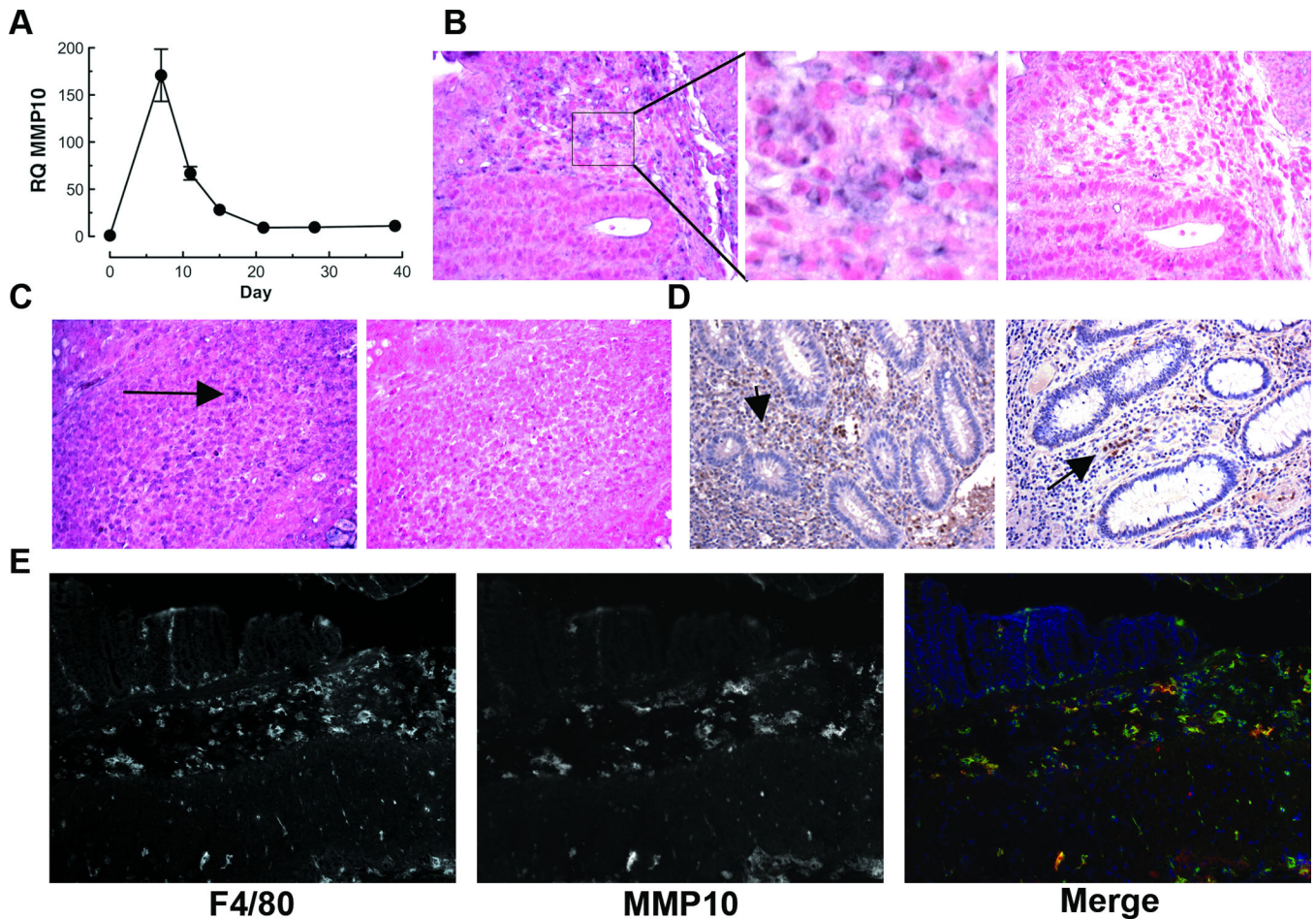


Fig 1. MMP10 is induced by inflammation in murine and human colonic tissue

(A) Real-time PCR analysis of MMP10 expression in colon tissue of C57BL/6 mice at different timepoints before, during and after a 7-day treatment with DSS. (B, C) *In situ* hybridization for *Mmp10* transcript in colon tissue specimens from DSS-treated (B) or *Il10*^{-/-} (C) C57BL/6 mice. Antisense and sense probes were both labeled with digoxigenin and applied at the same concentration. Positive signal is purple (e.g. arrows); nuclei are counterstained with Fast Red. A higher magnification of the area bounded by a rectangle in the DSS anti-sense image is shown in the adjacent panel. (D) Immunohistochemical detection of MMP10 protein in specimens of colon tissue from 2 different IBD patients. Positive signal is brown; nuclei are counterstained blue with hematoxylin. (E) Immunofluorescent co-staining of a frozen section of colon from a mouse after a 7-day treatment with DSS. The murine macrophage marker F4/80 is shown on the left, MMP10 is shown in the center and merged image showing F4/80 (green), MMP10 (red) and nuclear stain (blue) is on the right.

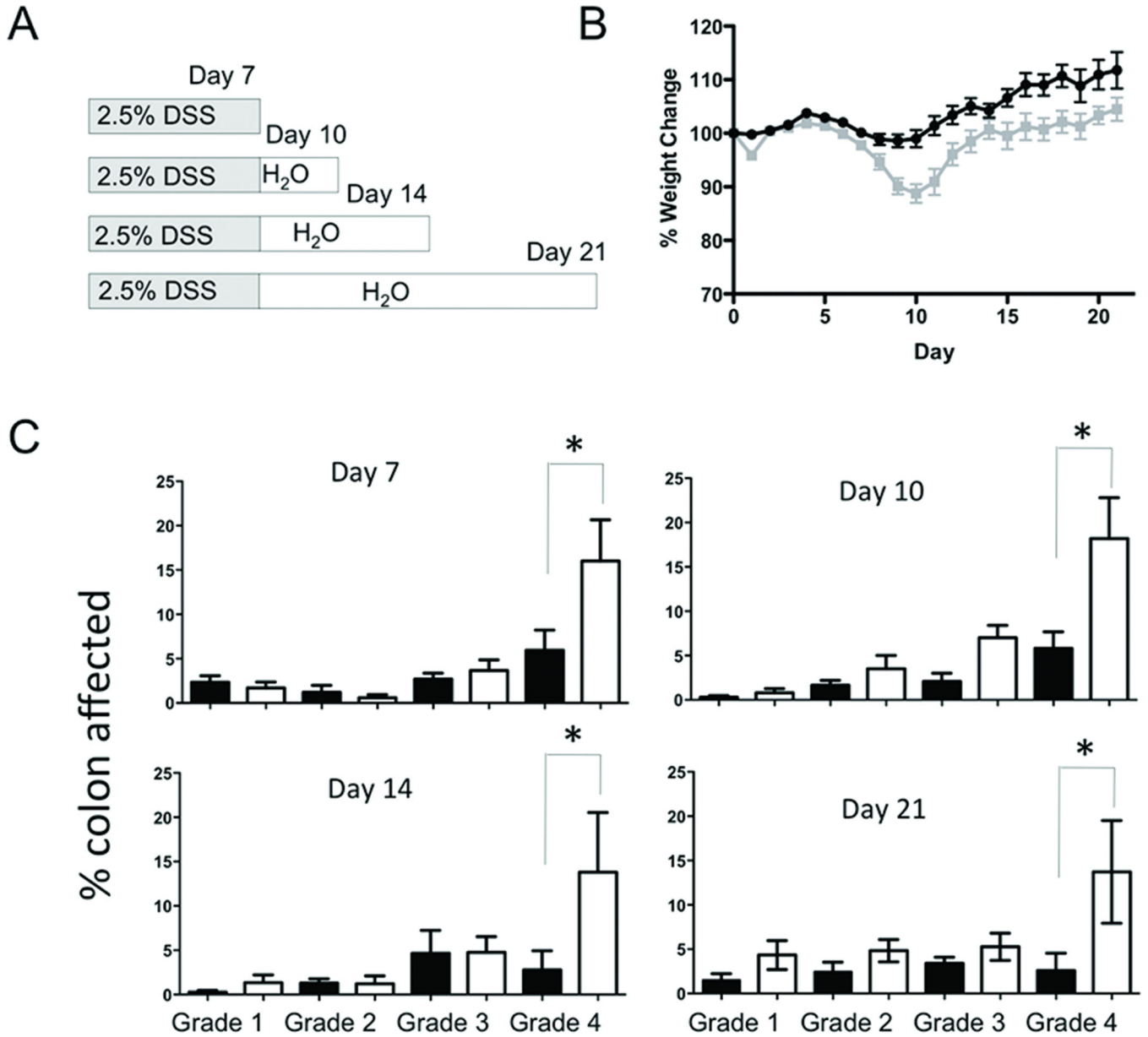


Fig 2. MMP10-deficient mice are significantly more injured by DSS treatment than wildtype mice

(A) Scheme showing the four timepoints after a 7-day exposure to 2.5% DSS at which cohorts of mice were analyzed. (B) Average weight change, relative to each individual starting weight, for all mice on the DSS protocol. Wildtype mice are shown in black, whereas *Mmp10*^{-/-} mice are in grey. (C) Histological scores for wildtype (black bars) and *MMP10*^{-/-} (white bars) colon sections from mice assessed at the 4 different timepoints outlined in (A). The description for each of the grades is given in the Materials & Methods. Shown is the average percentage of the colon length assessed at each grade for each group of mice.

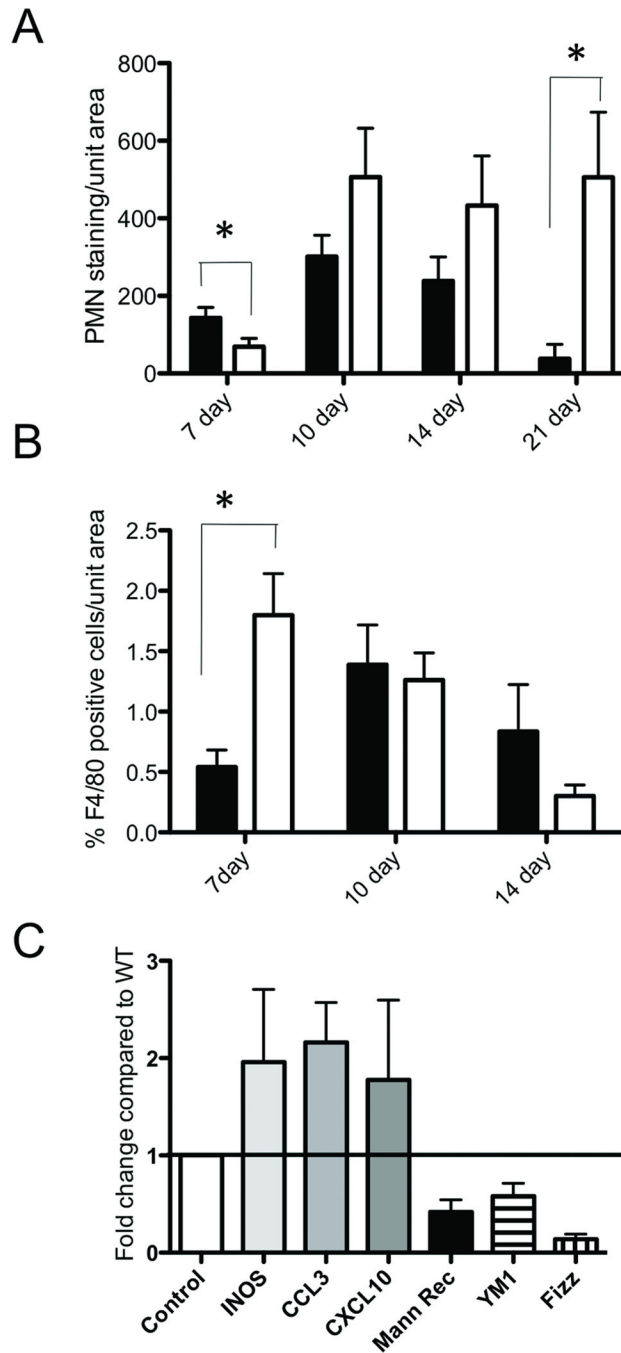


Fig 3. Leukocyte recruitment is altered in DSS-treated MMP10-deficient mice
 (A) The average level of PMN immunostaining per unit area of colonic tissue in wildtype (black bars) or MMP10^{-/-} (white bars) mice at each of the 4 timepoints after DSS treatment. (B) The average number of F4/80-positive macrophages per unit area of colon tissue from wild-type (black bars) or MMP10^{-/-} (white bars) mice at 3 timepoints after DSS treatment. Macrophages were undetectable at 21 days. (C) Whole colon lysates from 7-day DSS-treated mice were analyzed by realtime PCR for markers of macrophage activation status. Shown are the levels of markers of M1 macrophages (INOS, CXCL3 and CCL10)

and M2 macrophages (mannose receptor, Fizz and Ym1) in MMP10-null colons compared to levels in wild-type colons after normalization using levels of GAPDH.

Author Manuscript

Author Manuscript

Author Manuscript

Author Manuscript

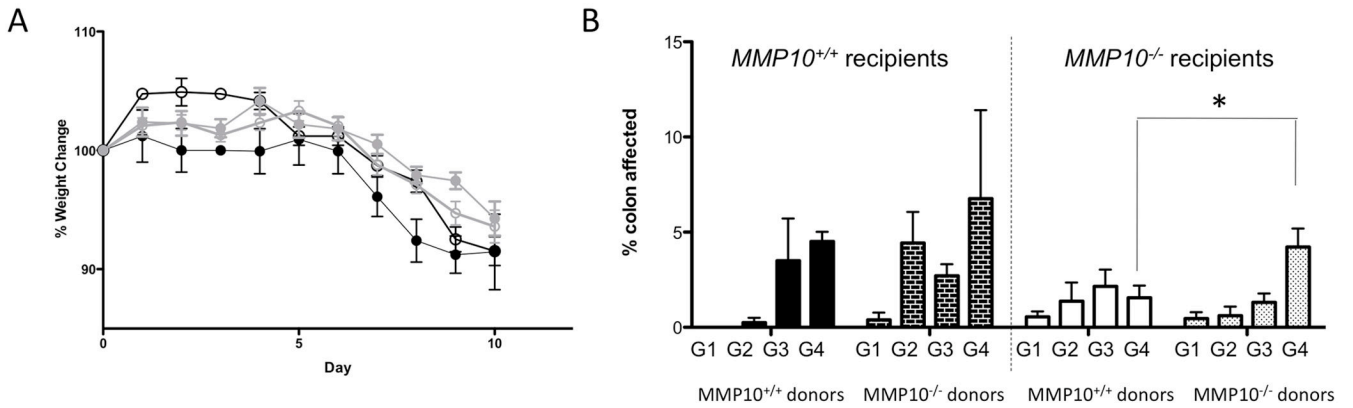


Fig 4. Bone marrow transplant experiments suggest colitis severity is largely controlled by bone marrow-derived MMP10

(A) Weight changes over the course of DSS treatment and 3-day recovery. Black symbols indicate wildtype recipients, while grey indicates MMP10^{-/-} recipients. Filled circles indicate wildtype donors, while empty circles indicate MMP10^{-/-} donors. (B) Histologic grades of colonic tissue specimens from bone marrow transplant mice. The dark bars on the left indicate wildtype recipients, while the light bars on the right are MMP10^{-/-} recipients. Solid bars are wildtype donors and hashed bars are MMP10^{-/-} donors. The grades (assigned as described in Materials & Methods) are indicated by G1 through G4, with the bars representing the average percentage of colon length calculated for each grade in each group of mice.

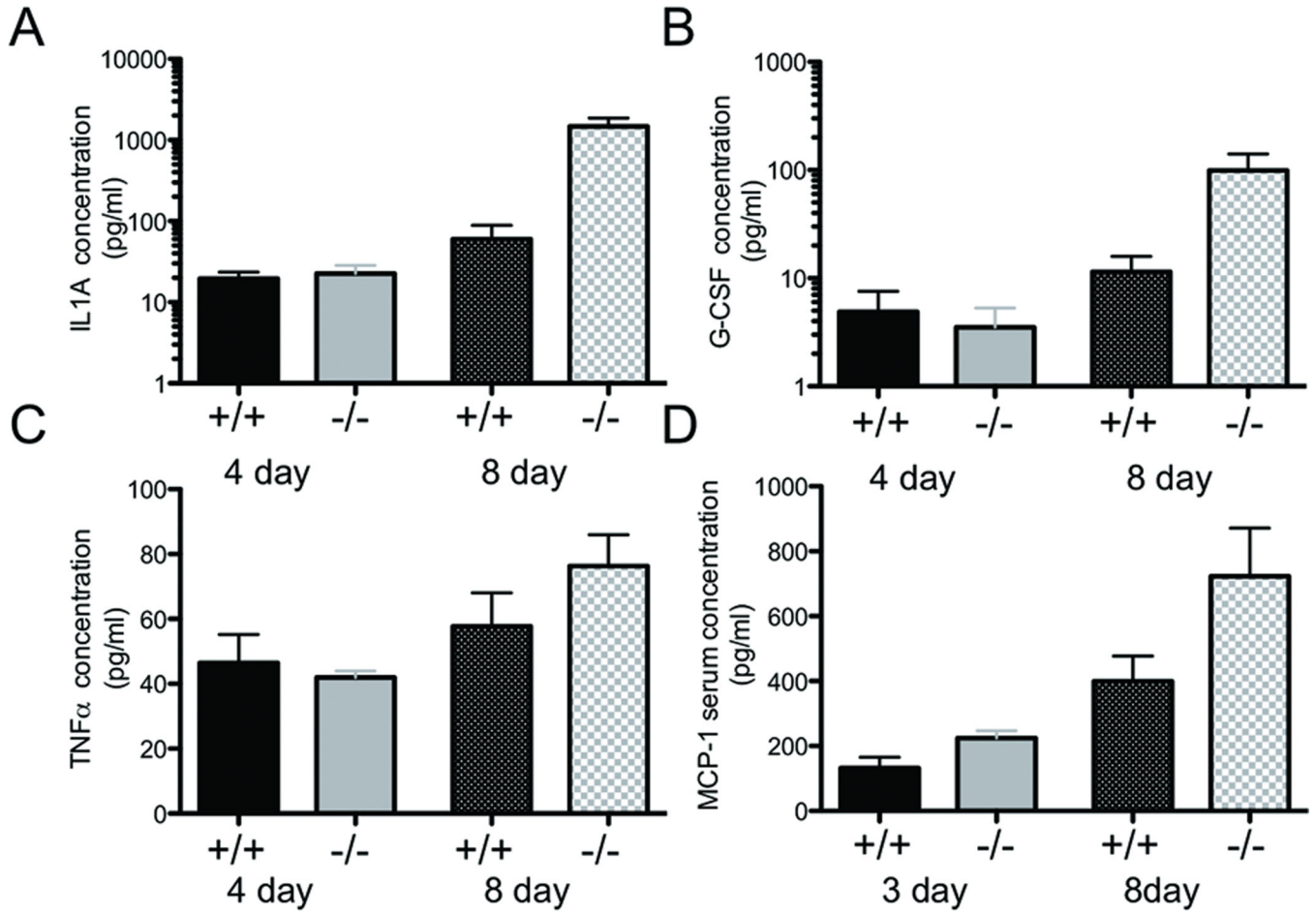


Fig 5. Levels of cytokines and chemokines detected by ELISA in fluids from DSS-treated mice
Levels of IL1a (A), G-CSF (B), and TNF α (C) measured in colonic lavage samples collected from mice on day 4 or day 8 of a 7-day DSS treatment protocol. Day 8 mice had one recovery day before collection. (D) Levels of the chemokine MCP-1 detected in serum from mice on day 3 or day 8 of a 7-day DSS treatment protocol.

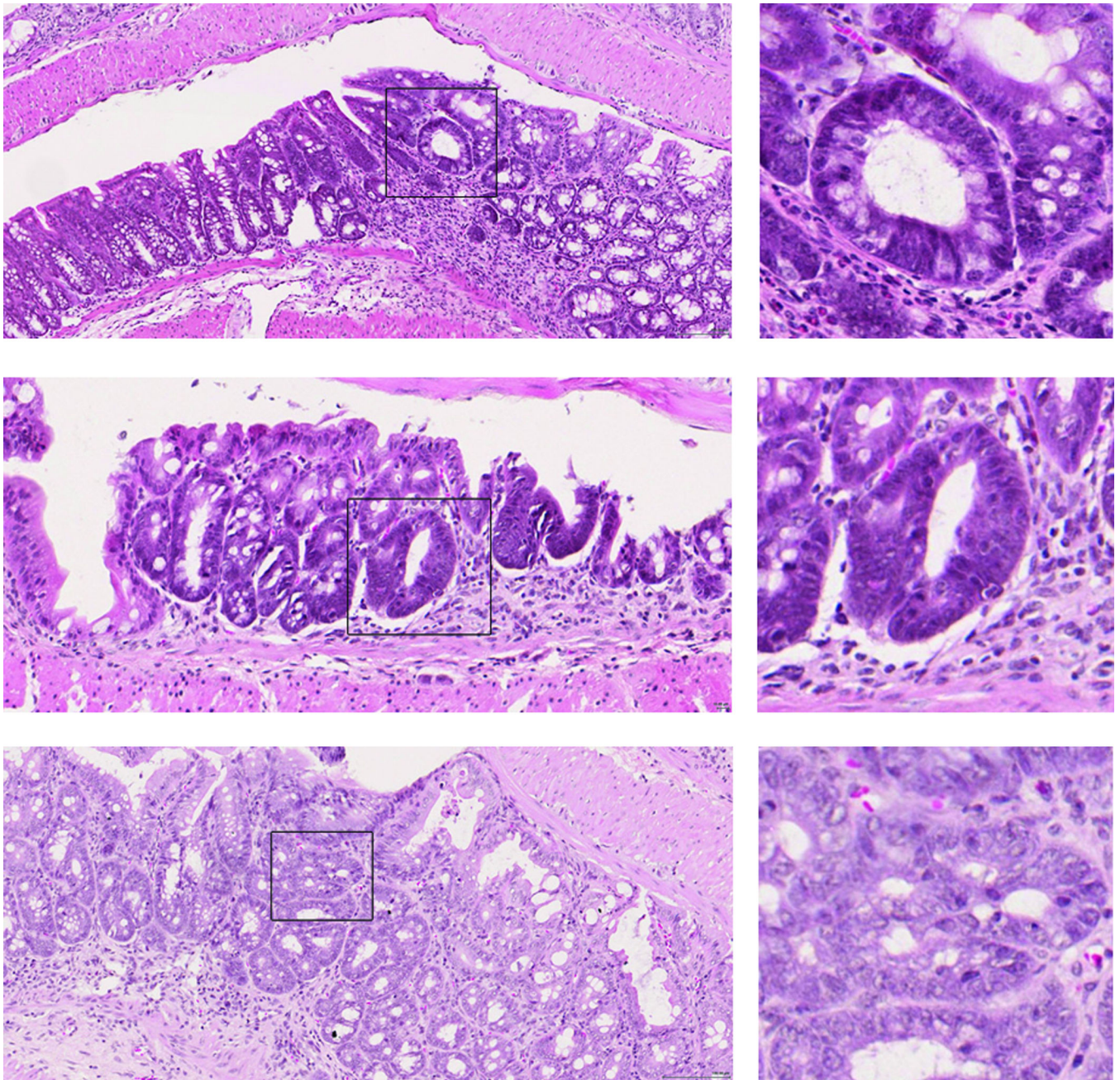


Fig 6. Dysplastic lesions are present in the colons of $MMP10^{-/-}$ mice after two rounds of DSS treatment

Shown are examples of hematoxylin and eosin-stained lesions from 3 different $MMP10^{-/-}$ mice. Boxed regions showing examples of dysplastic lesions are shown in higher magnification on the right. Scale bar = 100 μ m.